

Powder Metallurgical Tungsten Fiber-Reinforced Tungsten

JASPER Bruno^{1,a,*}, COENEN Jan W.^{1,b}, RIESCH Johann^{2,c},
HÖSCHEN Till^{2,d}, BRAM Martin^{3,e} and LINSMEIER Christian^{1,f}

¹Forschungszentrum Jülich GmbH, Institut für Energie- und Klimaforschung – Plasmaphysik, 52425 Jülich, Germany, ²Max-Planck-Institut für Plasmaphysik, 85748 Garching, Germany, ³Forschungszentrum Jülich GmbH, Institut für Energie- und Klimaforschung – Werkstoffsynthese und Herstellungsverfahren, 52425 Jülich, Germany

^ab.jasper@fz-juelich.de, ^bj.w.coenen@fz-juelich.de, ^cjohann.riesch@ipp.mpg.de,
^dtill.hoeschen@ipp.mpg.de, ^em.bram@fz-juelich.de, ^fch.linsmeier@fz-juelich.de

Keywords: tungsten, fusion, composite, powder metallurgy

Abstract

The composite material tungsten fiber-reinforced tungsten (W_f/W) addresses the brittleness of tungsten by extrinsic toughening through introduction of energy dissipation mechanisms. These mechanisms allow the release of stress peaks and thus improve the materials resistance against crack growth. W_f/W samples produced via chemical vapor infiltration (CVI) indeed show higher toughness in mechanical tests than pure tungsten. By utilizing powder metallurgy (PM) one could benefit from available industrialized approaches for composite production and alloying routes. In this contribution the PM method of hot isostatic pressing (HIP) is used to produce W_f/W samples. A variety of measurements were conducted to verify the operation of the expected toughening mechanisms in HIP W_f/W composites. The interface debonding behavior was investigated in push-out tests. In addition, the mechanical properties of the matrix were investigated, in order to deepen the understanding of the complex interaction between the sample preparation and the resulting mechanical properties of the composite material. First HIP W_f/W single-fiber samples feature a compact matrix with densities of more than 99% of the theoretical density of tungsten. Scanning electron microscopy (SEM) analysis further demonstrates an intact interface with indentations of powder particles at the interface-matrix boundary. First push-out tests indicate that the interface was damaged by HIP.

Introduction

For the first wall of a fusion reactor unique challenges are present requiring advanced materials in areas ranging from mechanical strength to thermal properties. The main challenges include wall lifetime, erosion, fuel management and safety. For the lifetime of the wall material, considerations of thermal fatigue as well as transient heat loading are crucial. Tungsten (W) is the main candidate material for the first wall of a fusion reactor as it is resilient against erosion by hydrogen isotopes, has the highest melting point of any element and shows good behavior under neutron irradiation [1]. One major disadvantage of W is its brittleness below the ductile-to-brittle transition temperature (DBTT), which ranges from 400-700 K [2], depending on the preparation history of the material. To circumvent the issue of brittleness when using W, different composite approaches are investigated. One example are tungsten laminates that consist of a stack of W foils which are assembled as a layer composite [3]. Tungsten fiber-reinforced tungsten (W_f/W), as another example, utilizes fiber-reinforcement and comprises of a pure W matrix and an interface layer around a W fiber [3,4]. W_f/W incorporates extrinsic toughening mechanisms that enable energy dissipation which leads to a reduction in stress peaks at crack tips and therefore cracks can be stopped. Accordingly, even in the brittle regime, this material allows for a certain tolerance towards cracking and damage in general in comparison to conventional tungsten.

In this contribution first results of the newly developed W_f/W samples produced with the powder metallurgical (PM) method of hot isostatic pressing (HIP) are presented in contrast to already existing CVI W_f/W [4]. Those were showing extrinsic toughening mechanisms similar to those of ceramic composite materials [5]. This mechanisms will also help to mitigate effects of operational embrittlement due to neutrons and high operational temperatures [1,5].

Composition of W_f/W . A W_f/W composite is composed of commercially available drawn tungsten fibers, coated with an interface layer and integrated into a W matrix. For testing single fiber samples are used (Fig. 1 Figure 1).

Different materials and material combinations were investigated as an interface material, e.g. copper, carbon and ceramics like erbia and zirconia [6].

The matrix of the first single fiber composite specimens was prepared using chemical vapor deposition (CVD). There tungsten hexafluoride (WF_6) is used, together with hydrogen, as the precursor gas. The composite is produced in a reactor in which the coated tungsten wires are aligned in the desired geometry and the precursor gas is fed through.



The WF_6 is reduced by the hydrogen in a heterogeneous surface reaction depositing the W metal on the interface of the fiber. In addition, multi-fiber composite samples were produced using chemical vapor infiltration (CVI), a special CVD technique. There the density of the samples can be optimized by means of the temperature profile together with the gas flow inside the reactor. Details are given in [4] and [7].

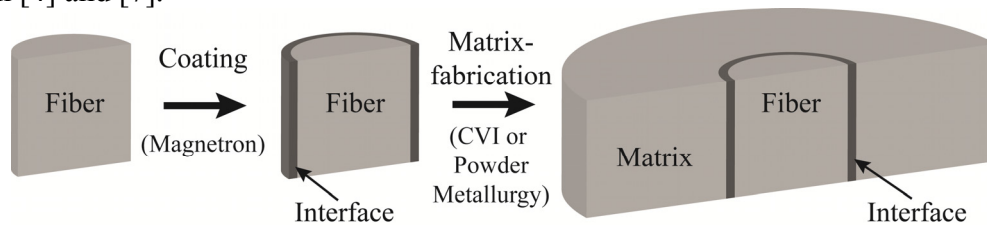


Figure 1: W_f/W consists of tungsten fibers, coated with an interface (e.g. Er_2O_3) and the W matrix.

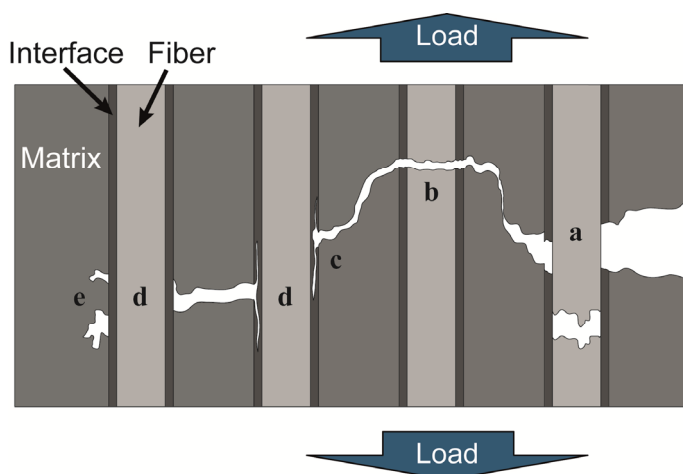
Even though production by means of CVI is straightforward, application of this method to large-scale prototypes and industrial application may prove difficult. In addition to further development of the CVI technology, we aim at an alternative production process that enables us to produce larger scale W_f/W samples in shorter time with the same properties.

For this reason HIP is chosen, where a green body of W powder is compacted at high temperatures and pressures to establish a final product close to the theoretical density. The main differences

between preparation via CVI and HIP are the acting forces and temperatures. For example the matrix of CVI tungsten is assumed to grow stress free and therefore its recrystallization temperature is higher when compared to powder metallurgically processed tungsten. During CVI there are no or little forces acting on the interface-fiber complex, whereas during HIP the samples are exposed to large forces, due to the external pressure. While during CVI a high level of densification is achieved (max 99%), it is unclear if a composite of maximum density of the matrix can be achieved via HIP.

Figure 2: A selection of energy dissipation mechanisms in a fiber-composite material. a) pull-out of fibers, b) pull-out of matrix elements, c) crack deflection at the interface, d) crack bridging by fibers, e) crack meandering at the interface

Therefore the interface acts as a barrier layer permitting the movement of the fiber with respect to the matrix (see Fig. 1). This enables the main energy dissipation mechanism in the composite, the pull-out of the fibers. Thermal stresses as well as compression of the tungsten powder, occurring



This is particularly important since for W_f/W and other composites relying on extrinsic toughening mechanisms the matrix–interface debonding behavior is a crucial factor.

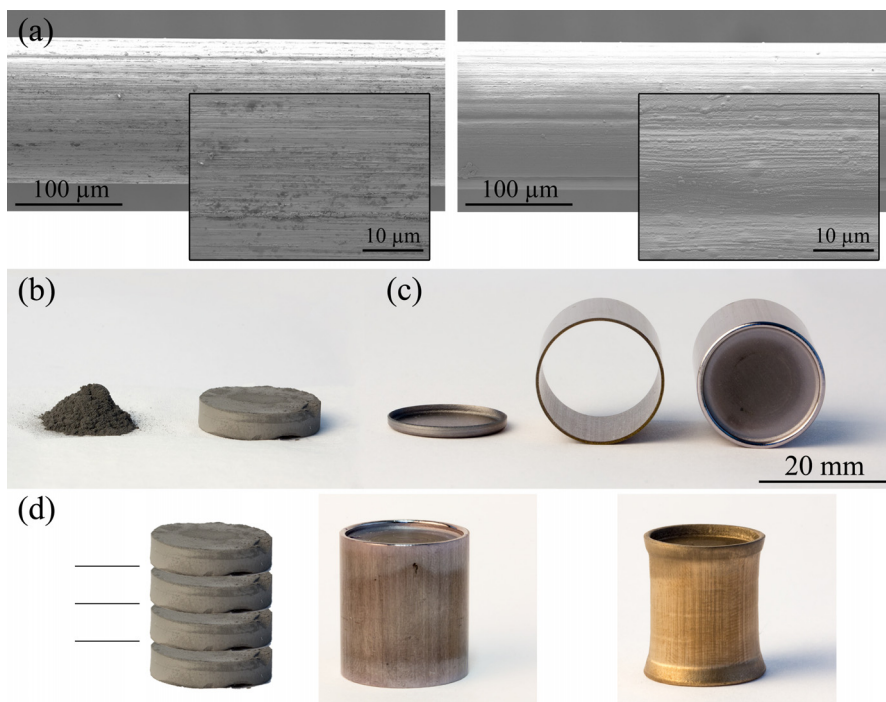
during HIP, have to be addressed as both can damage the fiber and interface and thereby diminish the available toughening potential.

Mechanical Properties of W_f/W . It was shown that W_f/W performed significantly better under mechanical loads than pure, bulk tungsten. Some of the mechanisms involved in the toughening are illustrated in Fig.2. They enable control of crack propagation through the dissipation of the respective energies by e.g. pull-out of the fibers or by crack propagation at the tailored fiber-matrix interface. Therefore, further propagation of the crack through the material is stopped [4]. Some level of interface optimization was achieved [6], further optimization with respect to the application in a fusion environment is foreseen. Most of the candidate materials are suitable to work as an interface when considering only mechanical properties, as all materials fulfill the debonding criterion [8]:

$$\frac{\text{fracture energy of the fiber}}{\text{fracture energy of the interface}} < 0.25 \quad (2)$$

To examine the interface behavior with respect to the debonding criterion a push-out test was used on single fiber samples [6]. 3-point bending tests on multi fiber samples were performed to investigate the mechanical behavior of the composite itself. These tests show that the fiber composite can withstand much higher loads than pure tungsten. Even after crack initiation it is still able to bear load, a clear indication that W_f/W is not prone to failure of full components [4]. Experiments, including synchrotron tomography, confirmed that the discussed mechanisms expected for energy dissipation in the composite system (see Fig. 2) are present [7].

Experimental Procedure



Powders. Two different powders provided by Plansee SE were chosen to produce the PM W_f/W samples. The mean particle diameter of the powders is 10.9 μm and 7.7 μm .

Fibers. The fibers used for this work are pure tungsten with a diameter of 150 μm (made available by Osram GmbH) and possess a tensile strength of typically 2900MPa and are not stabilized against recrystallization by potassium doping, hence typically losing their ductility when exposed to temperatures above 1000°C. For the integration into the HIP single fiber composite they are cut into pieces of 10mm. Due to the

Figure 3: Pictures of the steps of the sample preparation. (a) Pure W fiber (left) and coated with erbium oxide (right) (b) W-powder and pressed tablet (c) lid, rod and electron beam welded Ta capsule (d) montage of tablets and fibers, HIP-ready capsule and HIPed capsule.

production via drawing of the fibers they are of even thickness, feature an elongated, fine grain structure but can possess some roughness at the surface.

Hot Isostatic Pressing (HIP) - Sample Preparation. Some steps have to be taken into account before the final densification of the specimens with HIP can take place. First, the fibers are straightened with a constant force of 50N. This assures a well-defined and reproducible condition of the fibers. (Fig. 3a)

Second, a $1\ \mu\text{m}$ erbium oxide (Er_2O_3) interface is deposited onto the fibers in a magnetron sputter device, using 450W radio-frequency power on an erbium target in an Ar- O_2 atmosphere. A homogenous thickness of the interface is achieved by coating the fibers from both sides. Before coating, the fibers are plasma cleaned to assure the removal of any oxide at the surface.

Third, Tantalum with 99.9% purity (OSNABRUEGGE) is used as the capsule material, as there are no intermetallic phases between Ta and W [9]. For that purpose Ta tubes with an inner and outer diameter of 19mm and 20mm, respectively, are cut into cylinders of 22mm length. The necessary lids are stamped out of a Ta plate with a thickness of 0.5mm and electron-beam welded into the Ta cylinders to form the capsules. (Fig. 3c)

The last part is the fabrication of the powder green body via die molding. For this purpose the powder is filled into a die and is subsequently compressed at 106MPa for 1.5min into tablets of 4.3-4.5mm in heights and a diameter of 19mm (Fig. 3b). This results in an average green density of 52% of the theoretical density of W ($19.250\text{g}/\text{cm}^3$). Due to this procedure, the density of neighboring tablets can differ by 0.5%. Details are given in Table 1.

One or two fibers are then placed either between two tablets or, already during die molding, inside a tablet. Since there are no visible differences in the corresponding cross-sections of the respective samples, we will not further differentiate between both types of fiber integration. Finally, the tablets are put into the capsule and the second lid is electron-beam welded onto the capsule.

Hot Isostatic Pressing (HIP) – The Process. The samples presented in this work are hot isostatically pressed (HIPed) in an argon atmosphere at 200MPa for 4h, if not indicated otherwise. Carbon heating filaments are used to achieve the desired temperatures of 1600°C , 1700°C and 1900°C . The HIP run of three pure W samples, namely H701, H702 and H902 was stopped after 3h 7min and 28s, caused by a steady temperature rise in the heating zone of H701 and H702 from 1759°C to 1826°C . The HIP temperature of H902 was not affected.

Methodology. Before analysis, all samples were wire eroded and wire cut into pieces, appropriate for the specific analysis method. In addition, after cutting all samples are polished with a Saphier 550 - Rubin 520 polishing machine (ATM GmbH) using silicon carbide paper and $3\ \mu\text{m}$ and $1\ \mu\text{m}$ diamond polishing suspensions for the final polishing steps. The etching method 98c from the ASTM E407 standard for pure tungsten is used to reveal the grain structure [10].

All scanning electron microscopy (SEM) images are either taken with a DSM 982 Gemini or a Crossbeam 540 Gemini II (Carl Zeiss AG), which is also a focused ion beam (FIB) device. The density measurements are carried out on a pure W section of the sample after Archimedes' principle with a Cubis MSA225S scale and the density measurement kit YDK01 (Satorius AG). The grain size is determined following the ASTM E112 standard [11] (see Table 1).

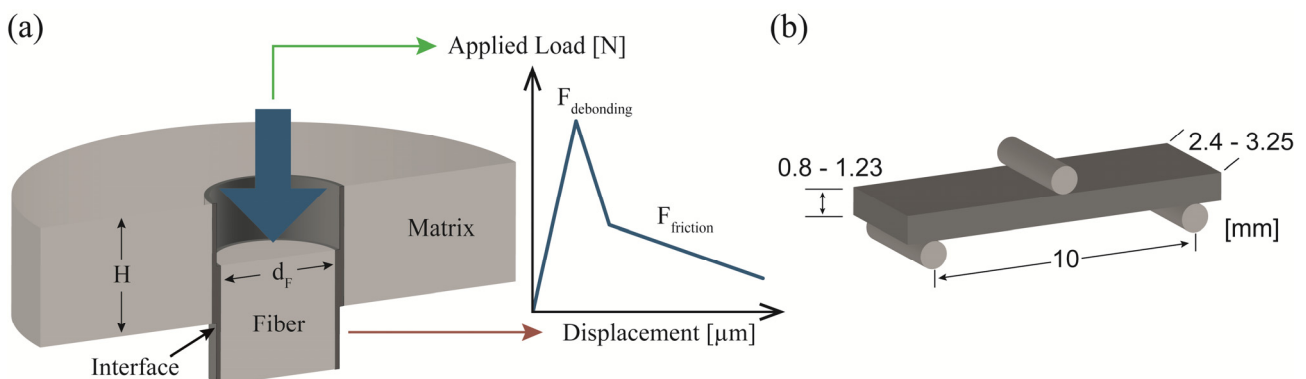


Figure 4: (a) Schematic drawing of the push-out test setup with the corresponding load-displacement curve. (b) Geometry of the 3-point bending test samples.

3-point bending tests for pure W matrix samples without fibers and push-out tests on single fiber samples are conducted using an Instron 3342 universal testing machine (Instron GmbH). For 3-point bending tests the support span is 10mm and the traverse velocity $0.5\text{mm}/\text{min}$. The sample geometry is shown in Fig. 4b. Since W is brittle at room temperature the obtained values follow a Weibull distribution [12]:

$$S(x) = \exp\left(-\left(\frac{x-\Theta}{\lambda}\right)^k\right) \quad (3)$$

Where k is the shape parameter, λ the scale parameter (measure of statistical dispersion) and Θ the location parameter (y-scale intercept) of the distribution.

Whereas the 3-point bending tests are performed on pure W samples, in push-out tests a micro-indenter is carefully placed over the fiber of a polished single fiber sample and a load-displacement curve is recorded (see Fig.4). This test gives insight into important parameters of the interface, e.g. the interfacial shear strength (τ_d). The corresponding load-displacement curve shows two important features, the frictional part and the maximum load which the sample is able to withstand before debonding. If this value is obtained for a number of specimens of the same batch, one can acquire τ_d by a simple fit according to [6]:

$$F_{\max} = \pi \frac{d_f \tau_d}{\alpha_2} \tanh(\alpha_2 \cdot H) \quad (4)$$

Where F_{\max} is the maximum load, d_f the diameter of the fiber, α_2 the elastic constant a parameter in the shear-lag theory, τ_d the interfacial shear strength and H the thickness of the sample.

Results

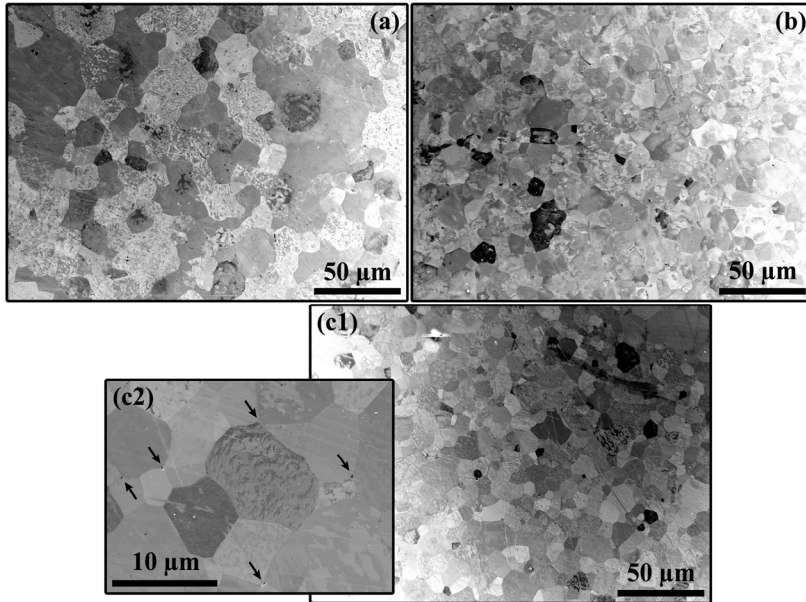


Figure 5: SEM secondary electron images of H902 (HIPed at 1900°C) (a) and 1792°C in (b), (c1) and (c2). Arrows mark small pores.

parameter k of $5,95 \pm 1,46$, a scale parameter λ of 744 ± 40 MPa and a location parameter Θ of $6,6 \pm 0,05$, were acquired (see Fig.6). For all tested batches, the obtained bending strengths show a broad range, a clear indication for a brittle material behavior.

Fibers. In SEM analysis of cross sections it is found that the diameter of the fibers is larger after HIP by as much as 10% and coarsening of the grain structure is observed. In addition, the grain structure is coarsened since non doped fibers were used.

Interface Parameters and Fiber Push-out. SEM analysis demonstrates an intact interface with indentations of powder particles at the interface-matrix boundary (see Fig.7). In addition, FIB analysis reveals that the erbium oxide of the interface forms a complicated 3D structure between the grains of the matrix.

Push-out tests performed on single fiber W_f/W samples result in an interfacial shear strength (τ_d) of 367 ± 48 MPa. The corresponding load-displacement curves are presented in Fig.7a. SEM analysis after the push-out test reveals failure of the matrix close to the interface region as can be seen in Fig.7b.

Matrix Parameters. The samples prepared at 1600°C and 1700°C exhibit a density of 99% of the theoretical density of W (19.250 g/cm^3 [13]), or higher. In the 1900°C case, the matrix has a density of 97.73%. Refer to Table 1 for details.

A dense matrix is also observed in SEM images of cross sections of all samples. In Fig.5 representative SEM images are presented. Small pores, in the order of 200nm, are detectable at triple points of grains (see Fig.5c2).

3-Point Bending Tests. The tests are performed for samples HIPed at 1600°C, 1700°C and 1900°C. A Weibull fit was done for samples compacted at 1700°C and a shape

Table 1: A list of important properties of the samples used in this work with the respective uncertainties in parenthesis

	H701	H702	H902	H6F01	H6F02	H7F01	H7F02
HIP Temperature [°C]	1759-1829 ^a	1759-1829 ^a	1900	1600	1600	1700	1700
HIP duration	3.12h	3.12h	3.12h	4h	4h	4h	4h
Mean powder particle size [μm]	7.7	10.9	10.9	10.9	10.9	10.9	10.9
Mean grain size after HIP [μm]	6.(0)	9.(6)	10.(5)				
Average green density before HIP [%]^{bc}				52.(1)	52.(2)	51.(7)	51.(9)
Density after HIP [%]^b	99.(4)	99.(2)	97.(7)	99.(3)	99.(5)	99.(6)	99.(6)

^a Temperature was rising monotonically from 1759 °C to 1829 °C, therefore the HIP run was stopped after 3h 7min and 28s, please refer to the text for more details; ^b In percent of the theoretical density of W (19.250g/cm³ [13]); ^c The local green density can vary by 0.5% from the average green density due to the preparation procedure.

Discussion

Matrix Properties. In 3-point bending tests samples of the pure W matrix showed brittle behavior as expected for W at room temperature or in general temperatures below the DBTT. The acquired Weibull distribution parameters with a scale parameter λ of 744MPa, for samples HIPed at 1700 °C, confirm this. They are also in the range of values found in literature for samples compacted under comparable conditions [14,15].

Density of HIP W_f/W . It was shown that it is possible to produce dense W and single fiber W_f/W samples via HIP. An analytical model by Redouani *et al.* for pure W predicts relative densities of

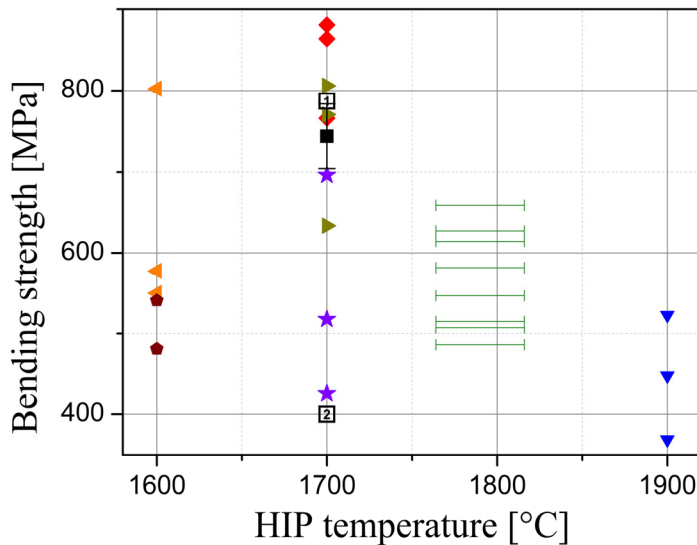


Figure 6: Bending strength for samples HIPed at 1600 °C, 1700 °C and 1900 °C. The scale parameter λ is 744MPa for the given samples at 1700 °C. For Details on H702 please refer to the text.

- ◀ H6F01-C
- ◆ H6F02
- ◆ H7F01-B
- ★ H7F01-C
- ▶ H7F02
- H702
- ▼ H902
- Aguirre *et al.*
- Song *et al.*
- $\lambda = 744$ MPa
 $k = 5,35$

only 94% and 97% for 1700 °C and 1900 °C, respectively after HIP for 4h at 200MPa [16]. This discrepancy could be explained by differences in the powder properties. The calculations by Redouani *et al.* are based on spherical particles of 10μm diameter, whereas in real powders, particles vary in geometry and also in size.

The lower density of the 1900 °C sample could be attributed to micro-leaks in the Ta capsule due to the high temperature. This would lead to argon ingress, which cannot be dissolved by the tungsten and therefore would result in pores and an incomplete densification.

Er₂O₃ Interface and Push-Out Tests. Powder particle indentations are visible in cross sections of the interface (see Fig.7). It seems therefore reasonable to assume that during HIP the powder particles of the matrix are pressed into the interface, which is in return squeezed between the grains of the matrix. This is supported by the fact that the thickness of the Er₂O₃ interface is less than the deposited 1μm before HIP and varies locally. This is a clear indication of the magnitude of the

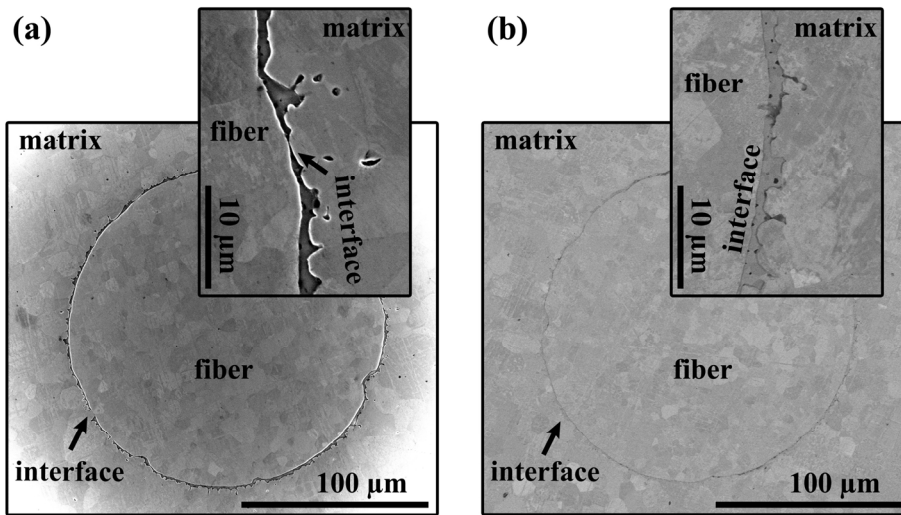


Figure 7: SEM pictures of cross section of W_f/W single fiber composites showing the intact but deformed interface. (a) Secondary electron (SE) image with good lateral resolution, sample HIPed at 1600°C (b) Back-scattered electron (BSE) signal for Z contrast, sample compacted at 1700°C

forces acting on the composite during HIP, which is also expressed by the increased diameter of the fibers after HIP. A reason could be the anisotropy of the geometry of the fibers, which in total leads to compression along the fiber axis and in return to swelling in radial direction. This also influences the behavior of HIP single fiber W_f/W samples during push-out tests. When compared to results obtained from CVD single fiber W_f/W samples with Er_2O_3 interface, $\tau_d = 367 \pm 48 \text{ MPa}$ is in the expected range of values of 399 MPa and 363 MPa for an interface thickness of $1 \mu\text{m}$ and $0.6 \mu\text{m}$, respectively [6]. Since push out of matrix elements was observed after the push-out tests it is not clear if complete debonding of the interface took place and therefore if the obtained shear stress can be attributed solely to the interface. To make final conclusions and provide the proof of principle that indeed HIP W_f/W shows a toughening effect when compared to pure W , more push-out tests of single fiber samples have to be performed.

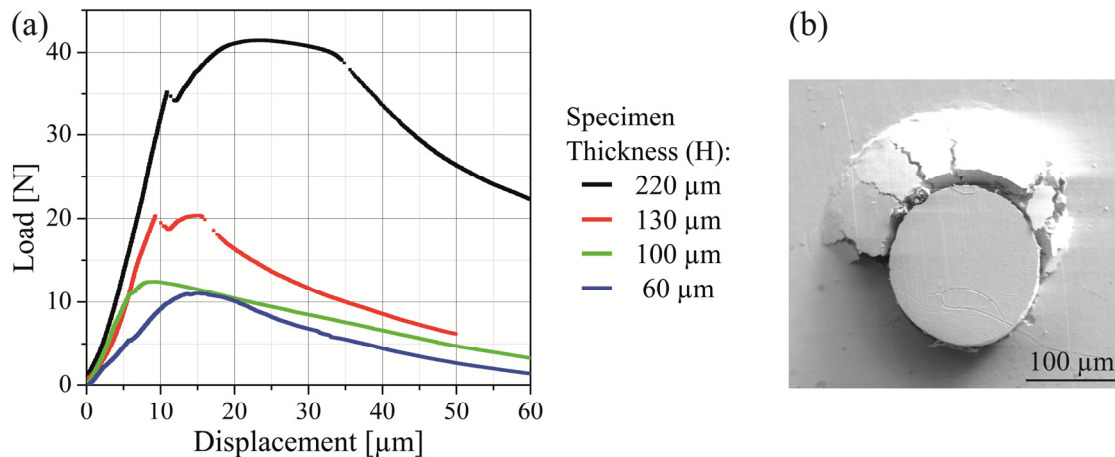


Figure 8: (a) Load-displacement curves of different specimens of one HIP single fiber W_f/W sample. (b) SEM picture of the pushed out fiber and failed matrix after the push-out test.

Conclusion & Outlook

First single fiber samples of the tungsten fiber-reinforced tungsten (W_f/W) composite material are produced via the powder metallurgical (PM) process of hot isostatic pressing (HIP). The samples demonstrate a dense matrix that displays brittle behavior in 3-point bending tests. Scanning electron microscopy (SEM) analyses reveal a deformed but intact interface after HIP. Push-out tests are performed to verify the operation of the expected debonding mechanisms. Since failure of the matrix occurred during the tests, more have to be performed to answer this question conclusively. This will allow a final verification if complete debonding at the erbium oxide interface takes place. Summarizing, the aim of both the chemical vapor infiltrated (CVI) W_f/W and the PM W_f/W development is a composite material with superior properties. Apart from matrix and fiber interaction, additional parameters come into play when fabricating a real multi-fiber composite. One

of those parameters is the fiber volume fraction of the material which has a major influence on the resulting mechanical properties of the composite.

A minimum fiber volume fraction has to be satisfied in any fiber composite before a strengthening effect is reached [17]. In addition, there is also a maximum possible fiber volume fraction beyond which no further incorporation into the matrix is possible. Concerning the tensile strength of a fiber composite, the maximum fiber volume fraction is also the optimal fiber volume fraction due to the fact that at this point every fiber can be utilized to its maximum capability [17].

Whether CVI or PM methods will be feasible to produce a W_f/W component has to be demonstrated by future experiments and further development.

Acknowledgements

A special thank goes to F. Koch, P. Zhao, W. Behr, R. Steinert and B. Coenen.

This work has been carried out within the framework of the EUROfusion Consortium and has received funding from the Euratom research and training programme 2014-2018 under grant agreement No 633053. The views and opinions expressed herein do not necessarily reflect those of the European Commission.

References

- [1] R. Lässer *et al.*, Structural materials for DEMO: The EU development, strategy, testing and modelling, *Fusion Engineering and Design*, 82 (2007) 511–520
- [2] H. Bolt *et al.*, Plasma facing and high heat flux materials-needs for ITER and beyond, *Journal of Nuclear Materials*, 307-311 (2002) 43–52
- [3] J. Reiser *et al.*, Tungsten foil laminate for structural divertor applications – Basics and outlook, *Journal of Nuclear Materials*, 423 (2012) 1–8
- [4] J. Riesch *et al.*, Enhanced toughness and stable crack propagation in a novel tungsten fibre-reinforced tungsten composite produced by chemical vapour infiltration, *Phys. Scr. T159* (2014) 014031 (7pp)
- [5] T. Hinoki *et al.*, Silicon Carbide and Silicon Carbide Composites for Fusion Reactor Application, *Materials Transactions*, 54 (2013) 472-476
- [6] J. Du, A feasibility study of tungsten-fiber-reinforced tungsten composites with engineered interfaces, Ph.D. Thesis, Technische Universität München, 2011
- [7] J. Riesch *et al.*, In-situ synchrotron tomography estimation of toughening effect by semi-ductile fibre reinforcement in a tungsten fibre-reinforced tungsten composite system, *Acta Mat.*, 61 (2013) 7060–7071
- [8] M.-Y. He, J.W. Hutchinson, Crack deflection at an interface between dissimilar elastic materials, *International Journal of Solids and Structures*, 25 (1989) 1053-1067
- [9] B. Predel, Ta-W (Tantalum-Tungsten), Madelung, O. (ed.), *SpringerMaterials - The Landolt-Börnstein Database*, DOI: 10.1007/10551312_2793 (15.02.02)
- [10] ASTM Standard E407, 1999, “Standard Practice for Microetching Metals and Alloys”, ASTM International, West Conshohocken, PA, 1996
- [11] ASTM Standard E112, 1996e3, “Standard Test Methods for Determining Average Grain Size”, ASTM International, West Conshohocken, PA, 1996
- [12] W. Weibull, *A Statistical Theory of the Strength of Materials*, Ingeniors Vetenskaps Akademien, 151 (1939)
- [13] E. Lassner, W.-D. Schubert, *Tungsten - Properties, Chemistry, Technology of the Element, Alloys and Chemical Compounds*, Kluwer Academic/Plenum Publishers, 1999
- [14] M.V. Aguirre *et al.*, Mechanical Behavior of W-Y₂O₃ and W-Ti Alloys from 25°C to 1000°C, *Metallurgical and Materials Transactions A*, 40 (2009) 2283-2290
- [15] G.-M. Song, Y.-J. Wang, Y. Zhou, Thermomechanical properties of TiC particle-reinforced tungsten composites for high temperature applications, *Int. J. of Refractory Metals and Hard Mat.*, 21 (2003) 1-12

- [16] L. Redouani, S. Boudrahem, Hot isostatic pressing process simulation: application to metal powders, *Canadian Journal of Physics*, 90 (2012) 573-583
- [17] N. Pan, Theoretical determination of the optimal fiber volume fraction and fiber-matrix property compatibility of short fiber composites, *Polymer Composites*, 14 (1993) 85-93